



# Topographic Analysis of Impact Craters on Enceladus and Ganymede: Evidence for Viscous Relaxation

Kelsi N. Singer (1), Michael T. Bland (1), William B. McKinnon (1), and P. M. Schenk (2)

(1) Department of Earth and Planetary Sciences and McDonnell Center for the Space Sciences, Washington University, St. Louis, MO 63130 (ksinger@levee.wustl.edu, mckinnon@wustl.edu), (2) Lunar and Planetary Institute, Houston, TX 77058.

## Abstract

Ganymede is the largest icy satellite yet no longer geologically active; Enceladus, though small, is currently active, and so holds valuable keys to understanding icy satellite tectonics and cryovolcanism. We examine viscously relaxed craters on these two bodies as a window into their thermal histories and the geologic activities associated with past heat flow. We take advantage of topographic information to constrain the shapes of viscously relaxed craters for two purposes: 1) to inform viscoelastic finite element studies of relaxation by providing realistic initial and final profiles of similarly sized craters [1], and 2) to ultimately produce maps of heat flow (for a given duration) for different portions of Ganymede's and Enceladus' surface.

## 1. Introduction

One advantage of studying craters is that we can estimate the initial shapes of craters and compare these to their present state to learn about their evolution. Craters on Ganymede and Enceladus display a range of relaxation states. While it is not possible to uniquely invert for a heat flow history from crater shapes alone, it is possible to test certain heat flow scenarios in a forward modeling sense [1].

## 2. Mapping methods

Presented here are the two highest resolution regions with topography generated to date (Fig. 1): a mid-latitude cratered region on the trailing side of Enceladus (centered at 2°N, 205°W; 70 m/px Cassini data), and Anshar Sulcus on Ganymede (centered at 12°N, 191°W; 152 m/px Galileo data). All measurements of crater shape were conducted in ArcGIS as described below. Basemaps and topography for Ganymede have previously been

mapped by [2]. Topography for Enceladus is currently being processed in collaboration with P. Schenk and O. White.

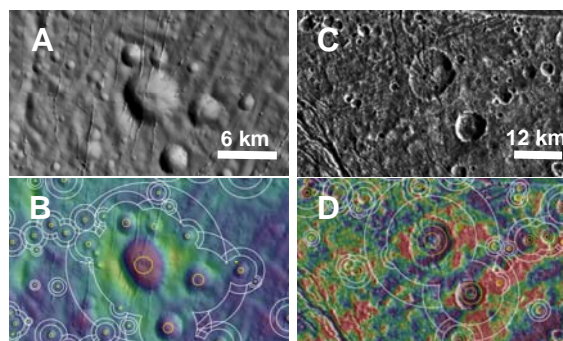


Figure 1: Elevation measurement technique for (a-b) Enceladus (stereo-controlled photogrammetry) and (c-d) Ganymede (photogrammetry only for this region).

### 2.1 Relaxed crater shapes

Similar to [3] we characterize the shape of the craters with the “relaxation fraction” ( $RF = 1 - d_{final}/d_{initial}$ ) using predicted initial depths and measured final depths of the crater. These depths ( $d$ ) are measured with respect to the level of the surrounding terrain (“apparent” depths). To estimate the level of the surrounding terrain we averaged the elevation values in a radial ring extending from one to two crater radii away from the rim (see Fig. 1), a range determined by experimentation. Additionally, any other obvious craters were excluded from each radial “donut”. The surface of Ganymede is quite rough at high resolution, but average elevations for the surrounding terrain well matched estimates from profiles across a given crater. The background terrain on Enceladus is generally smoother, although there are obviously many fractures on various scales, and the example region in Fig. 1a is crossed by several tectonic bands.

On Enceladus, the average elevation of the pixels in a circle 1/3 of the radius centered on the crater floor produced a depth that matched that estimated by profiling.

On Ganymede the elevation of the crater floors is quite variable. To obtain the depth of the relaxed craters we utilized two methods to obtain an upper and lower bound in a consistent manner across all craters. As an upper limit on  $d_{final}$  we used the lowest elevation anywhere inside the crater rim. In some cases, however, this lowest point was in another small crater in the floor, or in regions that are in shadow (in which case the topography is indeterminate). Thus we also averaged the elevation in a radial ring around the crater floor, to provide an effective lower limit on depth. The floor ring extends from 1/3 to 2/3 of the crater rim radius, thus excluding the central peak region and rimwalls. In many cases this also cuts out shadowed areas.

## 2.2 Initial crater depths

In order to estimate the initial depth of the mapped craters on Ganymede, we used the depth-to-diameter ratio ( $d/D$ ) found by [4] for fresh craters on Ganymede. These measurements are from the rim crest, while our measurements are from the level of the surrounding terrain. We use older, Voyager-based measurements of rim height on Ganymede [5] to correct for this to first order; our topographic maps also give rim heights of relaxed craters directly, albeit with some systematic uncertainty. Enceladus has fewer fresh craters, especially at the larger diameters, but the ensemble of crater depths itself can be used to estimate initial apparent depths (see below).

## 3. Results

Fig. 2 shows the apparent crater depths versus rim diameter for both study areas. For Ganymede,  $d_{final}$  is displayed as the average of the upper and lower limits described above. In some cases, the range of possible depths is large, reflecting the inherent uncertainty in making these measurements on variable terrain. The range of apparent depths only hints at the bimodality seen elsewhere on Ganymede [2], although most of our relaxed craters are smaller. The relaxation fractions are generally moderate. This is not necessarily unexpected for small craters on an area of ancient, cratered terrain such as near Anshar Sulcus, but such relaxation likely requires sustained heat flows in excess of  $50 \text{ mW m}^{-2}$  [3,6].

The range of apparent depths for Enceladus craters is broad (Fig. 2a), and indicates the sustained (or at least intermittently renewed) action of processes such

as viscous relaxation or plume fallout over time. The upper envelope of the depth distribution may indicate the apparent depths of fresh simple craters on Enceladus; a similar effect is seen with MOLA-derived crater depths on Mars [e.g., 7].

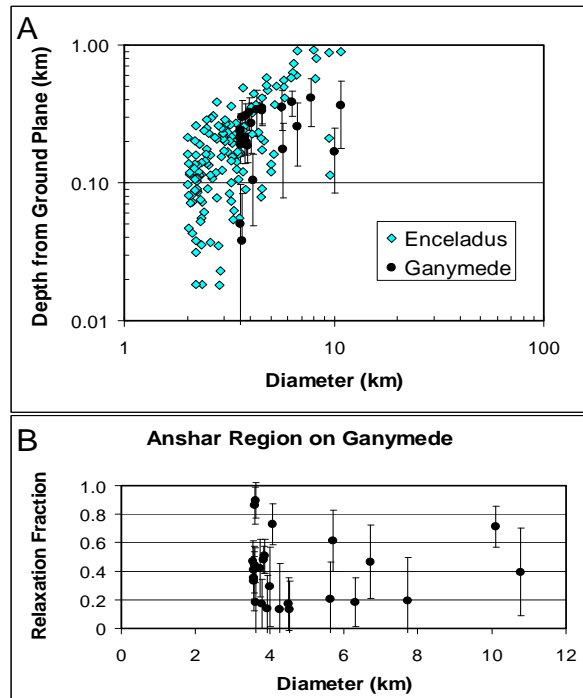


Figure 2: (a) Depth to diameter statistics for two high resolution study regions. (b) Relaxation fraction for the Anshar Region of Ganymede. Craters display a range of relaxation states.

## References

- [1] Bland, M., Singer, K., and McKinnon, W.: Enceladus' ancient heat flux: Clues from numerical simulations of crater relaxation. This conference, 2011.
- [2] Schenk, P.: The timing of viscous relaxation on Ganymede. LPSC abstracts, pp. 2083, 2010.
- [3] Dombard, A. and McKinnon W.: Elastoviscoplastic relaxation of impact crater topography with application to Ganymede and Callisto. Journal of Geophysical Research, Vol. 111, E1, pp. E01001, 2006.
- [4] Schenk, P.: Thickness constraints on the icy shells of the Galilean satellites from a comparison of crater shapes. Nature, Vol. 417, pp. 419-421, 2002.
- [5] Schenk, P., and McKinnon, W.: Estimates of comet fragment masses from impact crater chains on Callisto and Ganymede, Geophysical Research Letters, Vol. 22, 13, pp. 1829-1832, 1995.

[6] Bland, M., Singer, K., and McKinnon, W.: Constraints on Ganymede's thermal evolution from models of viscous relaxation. LPSC abstracts, pp. 1814, 2011.

[7] Boyce, J., et al.: Deep impact craters in the Isidis and southwestern Utopia Planitia regions of Mars. Geophysical Research Letters, Vol. 33, pp. L06202, 2006.